UCRL-ID-126780

Low-Frequency Electromagnetic Measurements as a Zero-Time Discriminant of Nuclear and Chemical Explosions-OSI Research Final Report

INIS-XA-N--329

Jerry J. Sweeney

December 1996

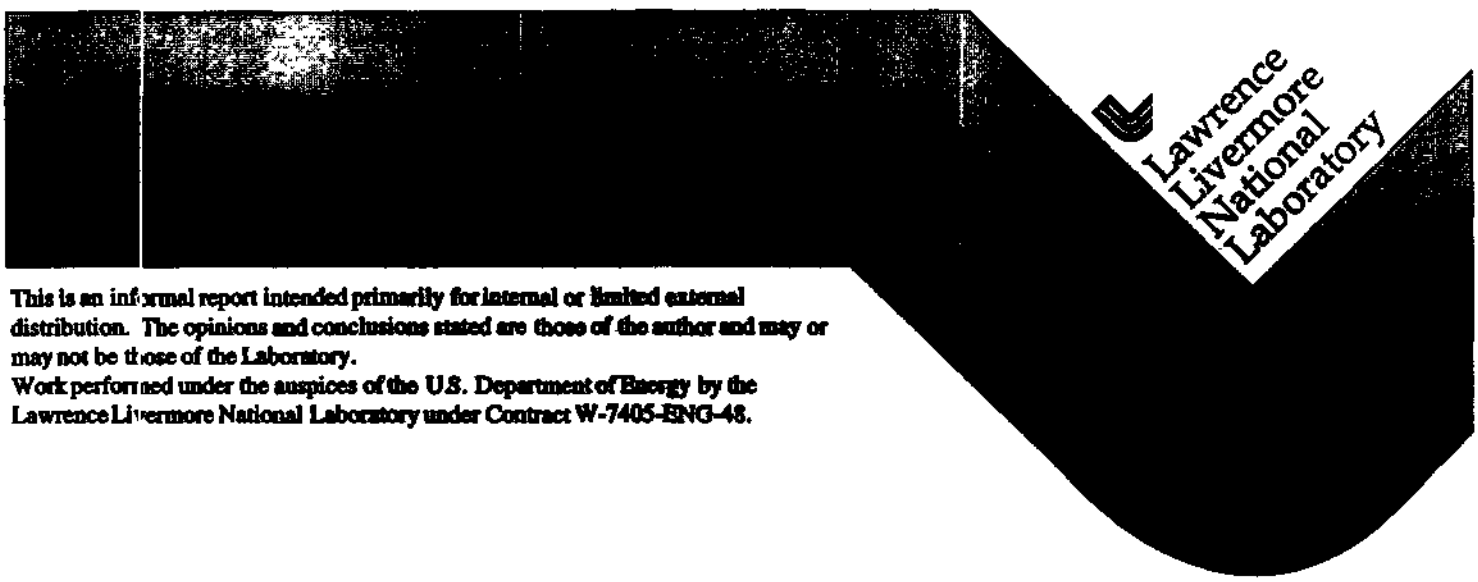

Work performed under the auspices of the U.S. Department of Energy by Lawrence Livermore National Laboratory under Contract W-7405-ENG-48.

Low-Frequency Electromagnetic Measurements as a Zero-Time Discriminant of Nuclear and Chemical Explosions-OSI Research Final Report

J.J. Sweeney

CTBT OSI Contract ST484B
Task 11.7.3 Deliverable

Low Frequency Electromagnetic Measurements as a Zero-Time Discriminant of Nuclear and Chemical Explosions–OSI Research Final Report

Jerry J. Sweeney
Lawrence Livermore National Laboratory

Abstract

This is the final report on a series of investigations of low frequency (1-40 Hz) electromagnetic signals produced by above ground and underground chemical explosions and their use for confidence building under the Comprehensive Test-Ban Treaty. I conclude that low frequency electromagnetic measurements can be a very powerful tool for zero-time discrimination of chemical and nuclear explosions for yields of 1 Kt or greater, provided that sensors can be placed within 1-2 km of the suspected detonation point in a tamper-proof, low noise environment. The report includes descriptions and analyses of low frequency electromagnetic measurements associated with chemical explosions carried out in a variety of settings (shallow borehole, open pit mining, underground mining). I examine cavity pressure data from the Non-Proliferation Experiment (underground chemical explosion) and present the hypothesis that electromagnetic signals produced by underground chemical explosions could be produced during rock fracturing. I also review low frequency electromagnetic data from underground nuclear explosions acquired by Lawrence Livermore National Laboratory during the late 1980s.

Introduction

The DOE Comprehensive Test Ban Treaty (CTBT) Research program was created to further knowledge about technologies that could be used for on-site inspections and confidence-building measures that may be called for under the provisions of the CTBT, which was signed by President Clinton in September 1996. The philosophy of the LLNL On-Site Inspection (OSI) project was to investigate technology areas which showed promise to be of great value for an OSI or confidence building, but were insufficiently understood. Four technologies, three of which apply to OSI and one which applies to confidence building, were identified for funding during FY95 and FY96. The OSI technologies are aftershock monitoring, noble gas transport modeling and sampling, and remote sensing of disturbed ground. This report covers the one confidence building technology–low frequency electromagnetic signals generated by underground nuclear and chemical explosions–and covers research activities during FY96 with a summary of current knowledge about the phenomena.

Low frequency electromagnetic (EM) measurements were first recognized as being a possible zero-time discriminant of nuclear and chemical explosions after the Non-Proliferation Experiment (NPE–see Sweeney, 1994). Measurements during the NPE at a distance of about 500 m from the 1 Kt chemical detonation suggested that the low frequency EM signature of a chemical explosion has longer duration, lower frequency content, and shows a delay from the detonation time compared to nuclear explosions. The objective of the FY95 and FY96 research program was to extend our experience with low frequency EM measurements to a wide variety of chemical explosion settings. During FY95, underground chemical explosions were monitored at the Henderson Mine (underground, hard rock) in Colorado, the Carlin Mine (open-pit, hard rock), and during the Kuchen readiness exercise (underground, borehole, small size, relatively shallow depths) at the

Nevada Test Site (NTS). The report by Sweeney (1995) gives the details of the mine measurements and preliminary results from the Kuchen experiment. Experience at Henderson Mine revealed difficulties involved with surface measurements of events occurring deep underground in a noisy mine environment. The Carlin experience indicated that the EM signal from a ripple-fired surface explosion is smaller than what would be expected from a single explosion equivalent in size to the total ripple-fired yield. Preliminary results of the Kuchen experiment indicated that the arming and firing circuitry can produce low frequency EM signals detectable at the surface near the borehole.

In this report, all the results of the Kuchen experiment are discussed along with results of two additional experiments carried out during FY96: measurements of several underground chemical explosions at the Linchburg experiment site in New Mexico and measurements done during a hydrofracturing experiment at the Lost Hills oil field in the southern San Joaquin Valley, California. The final section of this report contains a summary of our current understanding of the phenomena of low frequency EM generated by chemical and nuclear explosions.

Low Frequency Electromagnetic Measurements During the Kuchen Experiments, Nevada Test Site, June-September 1995

Introduction

During the summer of 1995 a series of three underground chemical explosions were detonated at Area 9, Yucca Flat, at the DOE Nevada Test Site. The purpose of these experiments was to study the near-field shock wave and seismic wave characteristics (i.e. study the source term) of a small (100 lb) chemical explosion detonated in alluvium. The experiments took place in three phases. In Phase I, 100 lb of explosive was detonated at a depth of 93 m, fully tamped in the borehole. For Phase II, the 100 lb explosion was detonated in a cavity, with the explosive at a depth of 64.5 m. Finally, in Phase III, the explosive was again detonated at 64.5 m, but this time the explosive was grouted in place to create a fully-tamped condition. All three phases of the test were carried out under conditions similar to those conducted during underground nuclear test conditions; field operations–including dry run pre-detonation practices and the use of similar arming and firing systems–were similar to those used during normal field test operations.

Because of above-ground activities and structures, I was able to site low frequency EMP sensors no closer that 20 m from surface ground zero for Kuchen. This gave a slant range of 95 m for Phase I and 67.5 m for Phases II and III. Three magnetometers and a vertical electric antenna were used as illustrated in Fig. 4 of Sweeney (1995). Because of all the equipment (trailers, generators, cables) in the vicinity of the site, I was unable to lay out the 50-100 m of wire in a straight line needed for a horizontal telluric line. The only change in the sensor system from that used in previous deployments was the use of an optical pre-amplifier for the vertical electric antenna which had not been tried in this system previously. This amplifier had a gain of 50 and, because it was optical, it provided very high input impedance with full electrical isolation.

There are some additional features of the Kuchen test that are relevant to electromagnetic signals. At the time of emplacement of the explosive, during Phase I and Phase II, and during all three dry run tests of the experiment, a large steel structure was in place over the emplacement hole. The mass of metal in this structure will move within the earth's magnetic field when the shock wave reaches the surface; this will create an induced magnetic field that may or may not be detected by the sensors or act as a reflector. This structure was removed during the last phase (Phase III)

of the experiment. The arming and firing circuits for this experiment were located at the surface. In the firing sequence, a capacitive discharge provides as much as 0.5 to 1 MW of electrical energy within a few microseconds to an exploding bridgewire which in turn ignites the high explosive. The charging and discharging of this circuit is another possible source of EMP. A signal is sent from the control room 90 seconds before detonation to arm the system. Typically, precise detonation times fall 60 to 70 ms after the exact hour or half-hour time chosen for the detonation. Thus, a typical detonation time (the time the bridge wire explodes) will look like 1300:00.062 UT (or local PDT), i.e. 0.062 s after the exact hour of 1300, and zero minutes. The detonations for Kuchen all took place in the early morning local time. This is an almost ideal situation for the EM measurements, since there is minimal wind noise at this time and higher mid-day atmospheric noise levels haven't yet been reached. In addition, the site is unusually quiet because equipment (generators, etc.) is turned off in the local area during detonation and personnel are cleared from the site.

Below, I discuss the results of the EM measurements from all three phases of the Kuchen series and the results of measurements taken during the dry run preceding Phase III. Rather than report these results in chronological order, I will start with a discussion of the dry run results, since these are vitally important for interpreting the data from all three phases when an explosion took place.

Dry Run for Kuchen III

Results from Phases I and II of the Kuchen series led me to suspect that the EMP observed was not coming from the underground explosion, but was related to some other source. In order to test the hypothesis that the source might be related to the arming and firing system, we operated the low-frequency electromagnetic sensors during the dry run prior to Phase III. During a dry run, the arming and firing sequence operates normally, except that current that normally goes to explode the bridgewires is routed into a dummy load. Thus, electrically, everything about the dry run should be the same as an actual detonation. For the ELF system, the important thing during a dry run is that there will be no ground motion from an explosion.

The dry run took place on August 30, 1995. During the dry run (and also during the Phase II and Phase III tests, but not during Phase I) a fiducial reference signal was also recorded at the ELF system on a separate channel of the Reftek digitizer. The fiducial signal was a derivative of the firing pulse that is used to explode the bridgewire. Because of the short duration of the pulse (microseconds), it was sent through a pulse stretching circuit before going to the Reftek. We also used the highest possible sampling rate in the Reftek (1000 Hz) in order to adequately sample the pulse. Our experience using this fiducial during Kuchen is that it gives an accurate reference for the detonation time of the explosive.

Figure 1 shows 140 s of data taken during the dry run. Traces for the magnetic and electric field signals in Fig. 1 show much more background noise than those shown below for other phases of Kuchen because the dry run took place during the later morning hours and personnel were still on site–a situation that doesn't exist when a detonation is carried out. In spite of the background noise, two distinct signals can be seen in Fig. 1: a pulse occurring 90s before detonation time seen in only the magnetic components, and a pulse occurring at detonation time seen in the magnetic components and in the vertical electric trace. The pulse occurring at detonation time in the magnetic components is actually a pair of pulses. Remember, there was no underground explosion in this case; these signals can only be attributed to the arming and firing system.

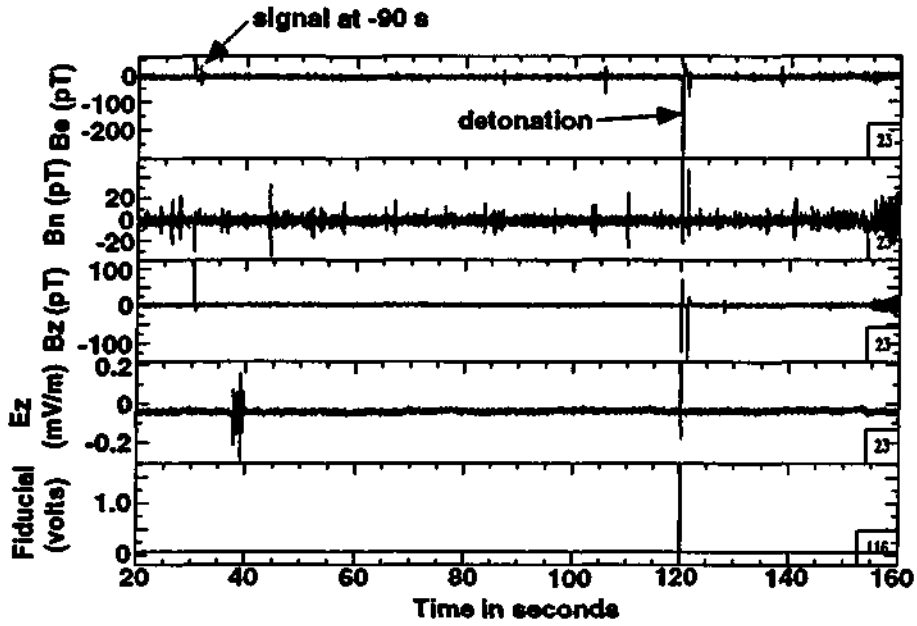

Figure 1. Signals recorded during the dry run for Kuchen Phase III, on August 30, 1995. A pulse is seen 90 s before detonation time in the three magnetic channels, but not on the vertical electric channel. A larger pulse is seen at detonation time on all three magnetic channels and on the vertical electric. The fiducial pulse gives a reference for the detonation time.

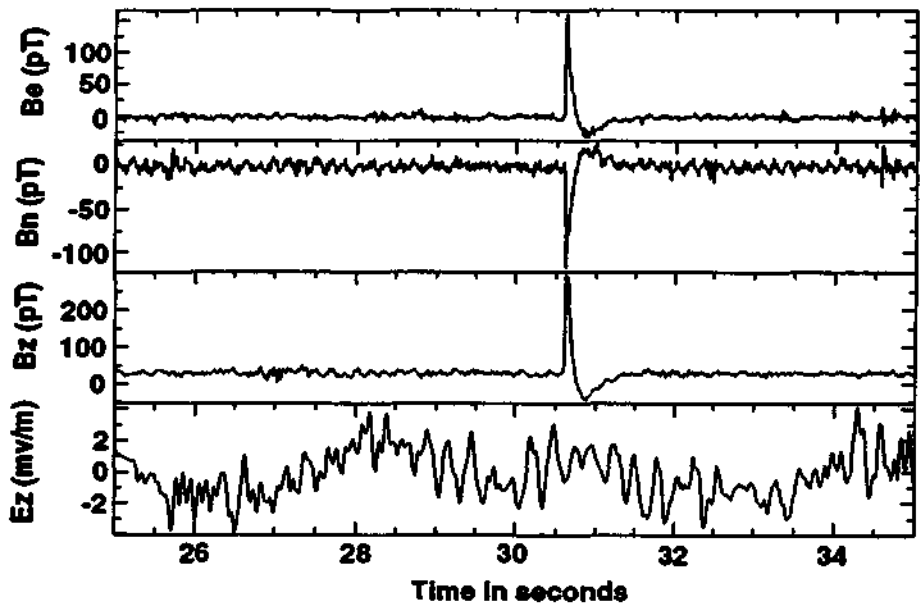

Figure 2. Expanded view of the pulse occurring 90 s before detonation during the Kuchen III dry run. No pulse is seen in the vertical electric component (bottom). The pulse seen on each of the three magnetic components is nearly identical to that seen 90 s before detonation for all three phases of Kuchen.

An expanded view of the early (90 s before detonation) signal is shown in Fig. 2. The pulse is seen to be less than 200 ms in duration with different magnitudes and phase among the three different components. The magnitude of this pulse–100-200 pT–is quite strong; these levels have a signal to noise ratio of more than 10-20. The pulse occurring at detonation time (in this case the firing signal is sent to a dummy load) is shown in detail in Fig. 3. Note that there are two pulses seen in the magnetic components, separated by about 2 seconds. In addition, the first of the two pulses occurs in the magnetic signals about 0.1 second or so before the detonation time, as shown by the fiducial. The pulse seen in the electric field signal occurs after the detonation time.

These results from the Kuchen dry run are extremely important for the interpretation of the data from the whole series. As will be seen below, the signals seen above during the dry run are all recognizable in the data from each of the three Kuchen tests.

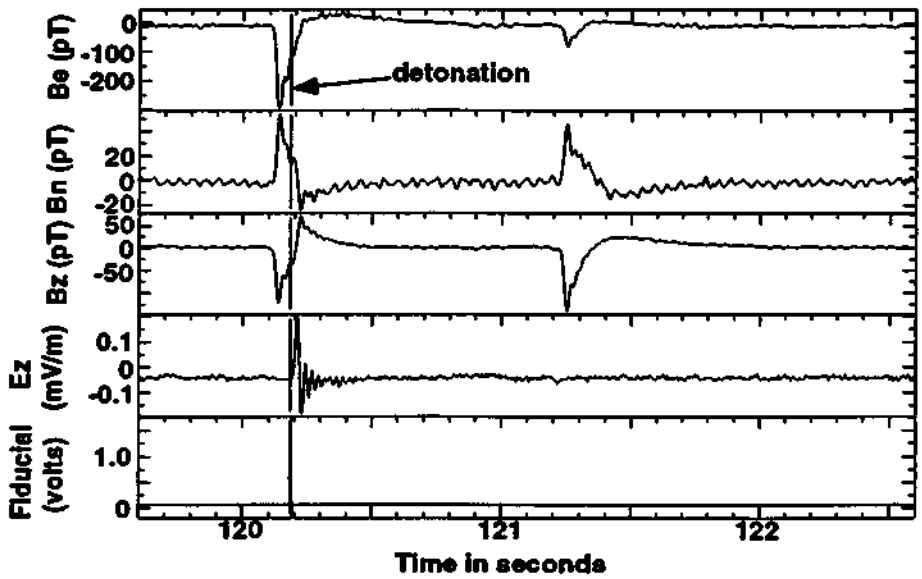

Figure 3. Expanded view of pulses occurring at detonation time during the Kuchen III dry run. The fiducial pulse marks the detonation time (when firing pulse is sent to the bridgewires). No explosion took place during this part of the test, the firing signal was sent to a dummy load.

Kuchen–Phase I, II, and III

The first phase of Kuchen was detonated at 0600:00.072 PDT on June 22, 1995. Initial results of the EMP measurements for Phase I were shown and discussed in Sweeney (1995). Here, we discuss additional insights gained after the conclusion of all of the tests, and especially, from results of the dry run discussed above.

A 300 s view of the data from Kuchen I is shown in Fig. 4. As in the case of the dry run, an EMP is seen both at detonation time and 90 s prior to detonation time. The pulse occurring 90 s before detonation is almost identical to that of Fig. 2. An expanded view of the later, detonation-time, signal is shown in Fig. 5. As seen in Fig. 3, there is a pulse appearing on the magnetic components with a roughly triangular shape that starts before the detonation time. (The detonation time was determined independently by the absolute timing of the signal sent to the bridgewires.) The

later part of the wave train, which is not seen in Fig. 3, is due to ground motion caused by the explosion arriving at the sensors. As the sensors move in the earth's static magnetic field, a signal is created. The caption for Fig. 5 notes the possible initial arrival of the ground motion about 70 ms after detonation time. This is an apparent wave velocity (for a slant range to the depth of the explosion of 95 m) of about 1360 m/s.

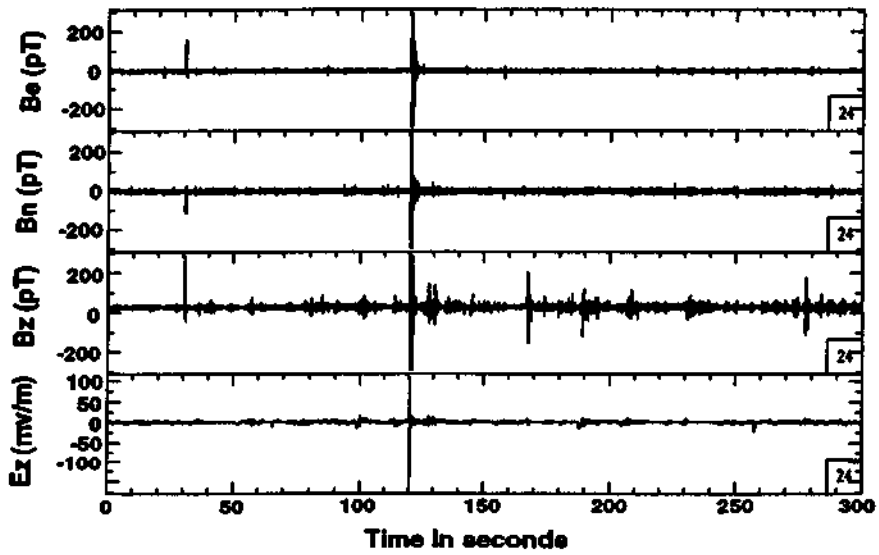

Figure 4. Low frequency EM data taken before and after detonation of Kuchen I. Detonation of the chemical explosive took place approximately at 120 s elapsed time. Note that the pulse occurring at approximately 30 s elapsed time is seen only in the magnetic components; it is related to the arming and firing signal. A fiducial reference timing pulse was not available during this phase of the experiment.

The same type of signals seen above for Kuchen I were seen for Kuchen II, detonated at 0600:00.069 PDT on August 10, 1995 and for Kuchen III, detonated at 0800:00.072 PDT on September 7, 1995. Pulses in the magnetic components 90 s before detonation virtually identical to those of Fig. 2 were observed for both Kuchen II and III. Signals occurring near detonation time for Kuchen II and Kuchen III are shown in Fig. 6 and Fig. 7, respectively

Figure 6 shows that the initial pulse arrived almost 100 ms (measured to be 84 ms) before detonation time. Arrival of the apparent ground motion at the sensors appears to occur very quickly after detonation–about 7 ms, for an apparent velocity of over 9 km/s–this is probably not due to ground motion at the site and may be related to other sources. Note in Fig. 6 that a second set of triangular-shaped pulses in the magnetic components is seen about 2 s after the initial pulse. This is similar to the case seen for the dry run in Fig. 3, so these pulses are also probably related to the arming and firing system. The shape of the pulse seen on the vertical electric channel indicates that the amplifier was saturated. The gain used in the amplifier is too high, but there may also be some additional problems with the preamplifier; I consider the electric data to be unreliable.

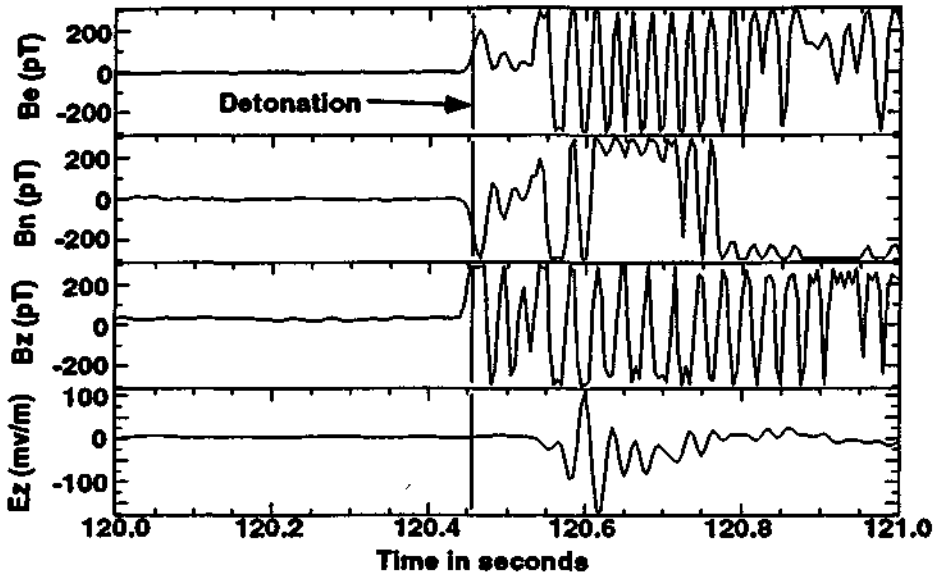

Figure 5. Low frequency EM signals near detonation time during Kuchen I. Detonation time (0600:00.072 PDT) is indicated by the vertical bar. Note that the first signal arrival precedes the detonation time in the magnetic components, similar to what was seen during the dry run (Fig. 3). A second pulse, seen on the east and north magnetic components, just when the electric signal starts and arriving about 70 ms after detonation, is due to ground motion arriving at the sensors.

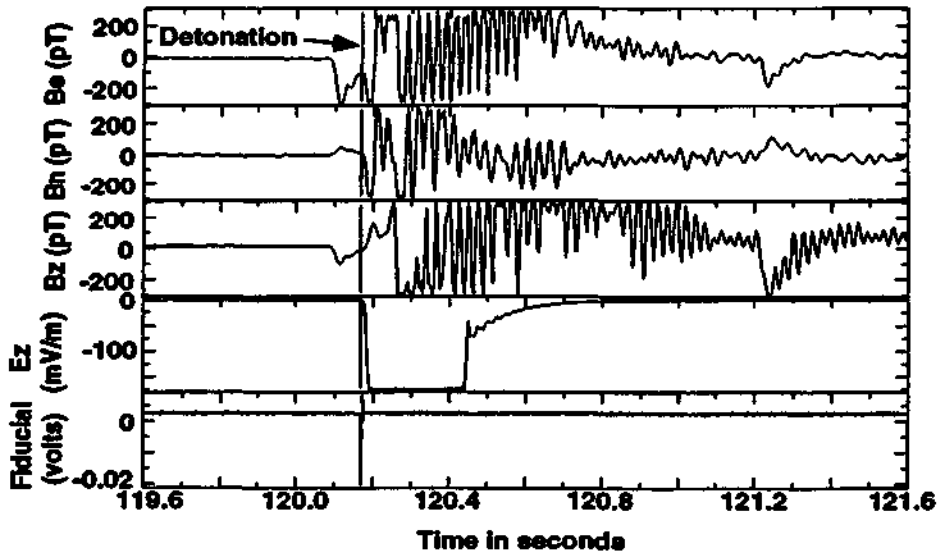

Figure 6. Low frequency EM data taken during the Kuchen II underground chemical explosion. Detonation time (see text) is indicated by a vertical bar. For this part of the test series, a fiducial signal was available to record the detonation time.

Figure 7 shows data for the Kuchen III test. The vertical electric channel was not operating properly for this part of the test series, so that data is not shown. In this case, the initial pulse occurs about 10 ms after the detonation time and a more vague second pulse, arriving one second later, can also be identified. This part of the signal is probably related to the arming and firing system, as discussed above. The rest of the signal is caused by ground motion, but it is difficult to assign a part of the signal to the first arrival of ground motion.

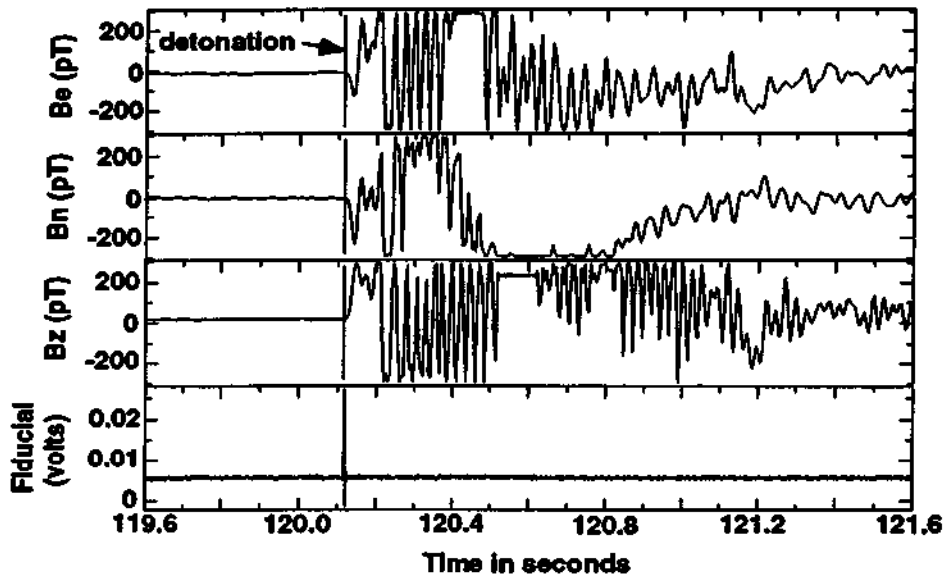

Figure 7. Low frequency EM data taken during the Kuchen III underground chemical explosion. Detonation time (see text) is indicated by a vertical bar and by the fiducial signal. The vertical electric channel for this test was inoperative.

Summary and Conclusions

The surprising result from the Kuchen series is that a significant low frequency EMP was apparently generated by the arming and firing system which, in this case, was located above ground. The signal related to the arming and firing system consists of three parts: (1) a short, triangular pulse occurring 90 s before detonation, (2) a longer duration triangular pulse occurring within ~100 ms of detonation time, and (3) a triangular pulse, similar to (2), occurring about 2 s after detonation. These pulses were seen for all three Kuchen explosions and during the one dry run that we monitored. These pulses, which are not related to the underground explosion, are of comparable amplitude (but very different pulse shape) to EMP we have observed at greater distances from larger underground nuclear explosions. The second pulse related to the arming and firing system masks any signal that may be produced during detonation of the explosive. The best we can say about any possible EMP from the explosion in this series of tests is that it probably was too small to be detected. This result would be consistent with estimates of the maximum standoff distance given by Sweeney (1995, Fig. 2).

What this experiment revealed is that the close-in electromagnetic environment of an underground explosion can be extremely complex. At ground zero there can be a strong above-ground source related to the arming and firing system, there can be additional sources due to movement of

metal structures by the shock wave, and there are many opportunities for reflections of signals from these sources from metal surfaces near ground zero. All this makes interpretation of the EMP very difficult, and further analysis of the Kuchen data is probably not warranted. Conditions used for the Kuchen series of explosions are not typical of most chemical explosion environments, but may be quite typical of an underground nuclear testing environment.

Linchburg Mine Experiments

Between late March and early May 1996, a series of underground explosive tests were carried out in the Linchburg mine near Magdalena, New Mexico. The experiments were a cooperative effort between the Waterways Experiment Station (WES), the Defence Nuclear Agency (DNA - now known as the Defence Special Weapons Agency - DSWA), LLNL, and Los Alamos National Laboratory (LANL). WES was responsible for the underground activities including execution of the detonations and some near-field gauge emplacements. DNA, LLNL, and LANL fielded surface seismic instrumentation in an experiment to study the source characteristics of the explosions. These detonations provided an excellent opportunity for us to field low-frequency electromagnetic instrumentation and add to our experience with underground explosions. The planned Linchburg experiments involved three detonations of composition B explosive, in the form of M15 land mines, ranging from 92.3 kg to 282 kg. In addition, there was an additional "waste" shot, involving about 2000 kg of explosives that were being disposed of, that we decided to monitor with low-frequency electromagnetic sensors because of its larger size. The dates of the detonations and size of charge in each case are given in Table 1.

The Linchburg mine is located a few miles south of Magdalena, New Mexico. The portal to the mine is located at an elevation of 8050 feet. The area where the detonations occur (chamber 1) is about 250 m from the mine portal and has about 100 m of overburden. The geology in the region consists of steeply-dipping layers of Paleozoic limestone and shale. There is a unit of Tertiary rhyolite and andesite located near the portal.

Table 1: Dates and size of charge for detonations at Linchburg Mine

Date	Size of charge
March 29, 1996	92.3 kg
April 4 1996	2000 kg
April 12, 1996	282 kg
May 9, 1996	282 kg

The mine is located on the steep western side of a north-south trending ridge with steep slopes near the portal. We chose two sites for the electromagnetic instruments at the surface which were as close as we could get to the underground detonations: one site at the portal (about 250 m away) and one site directly above the detonation point (referred to as site 1a) at an elevation of

about 8520 feet (about 143 m above the detonation point). At site 1a, an accelerometer was co-located with a north-south directed magnetometer and a vertical magnetometer. Data from all three instruments were sampled at 250 samples/s by a Reftek digitizer. At the portal site two magnetometers, oriented north-south and east-west, were installed about 20-30 m south of the portal. Data were also sampled at 250 samples/s at the portal site with a Reftek digitizer.

The explosive consisted of a pile of land mines located inside a cavity. For the explosions in March and April, the cavity was not sealed. The cavity was sealed for the detonation that took place in May. Based on estimates of the detection range versus yield given by Sweeney (1995), and the distances of the electromagnetic sensors from the detonation point (approximately 143 m and 250 m), all of the explosions except the 2000 kg one are small enough that we would not normally expect to see an electromagnetic signal. The 2000 kg explosion is close to the detection limit for the distances to our sensors. There is one additional consideration, however. Because these explosions take place in an open cavity, there is an opportunity for a larger fireball to develop than would be the case for a fully tamped explosion. If the size of the fireball affects the size of EM signal produced, then we would expect these explosions to have an enhanced EM signature and perhaps we might see a signal where we had not expected. As seen below, the results show that this is not the case; no zero-time signals were detected from any of the explosions, including the 2000 kg one.

Results of the detonation on March 29 are shown in Fig. 8. The figure shows data from the vertical accelerometer and vertical magnetometer at site 1a, directly above the detonation, and data from the two horizontal magnetometers located at the portal site. The signal from the horizontal magnetometer at site 1a is similar to that of the vertical magnetometer and is not shown here. There is no evidence of a zero-time signal on any of the magnetometers. The signal from the vertical magnetometer at site 1a closely tracks that of the accelerometer and comes from movement of the magnetometer in the earth's magnetic field. Similarly, the ground motion at the portal site is clearly seen, arriving slightly later than at site 1a because of the greater distance (there was no accelerometer emplaced at the portal site for comparison of ground motion). The large amplitude signal arriving about 1s after the ground motion at the portal site is caused by the sudden pulse of air forced through the tunnels by the explosion arriving at the portal. The later low frequency signal is probably caused by slow ground motion from the acoustic pulse arriving at the portal or by dust blowing out of the portal.

Signals recorded during the third (the second of the DNA-LLNL-LANL series) Linchburg mine detonation on April 12 are shown in Fig. 9. In this case the signals are almost identical to those of Fig. 8 except that amplitudes are slightly larger because the detonation was about three times larger. For the "waste" shot 2000 kg detonation of April 4, shown in Fig. 10, signal amplitudes are much larger, but in general show very little difference from those of Fig. 8 or 9. In both of the April explosions there was no evidence of a zero-time EMP. Signals from the last shot, which occurred on May 4, are not shown; signals from this shot also showed no zero-time signal and are nearly identical to those of Figs. 8-10 except that in this last case there was no air blast seen at the portal because the explosion chamber was sealed.

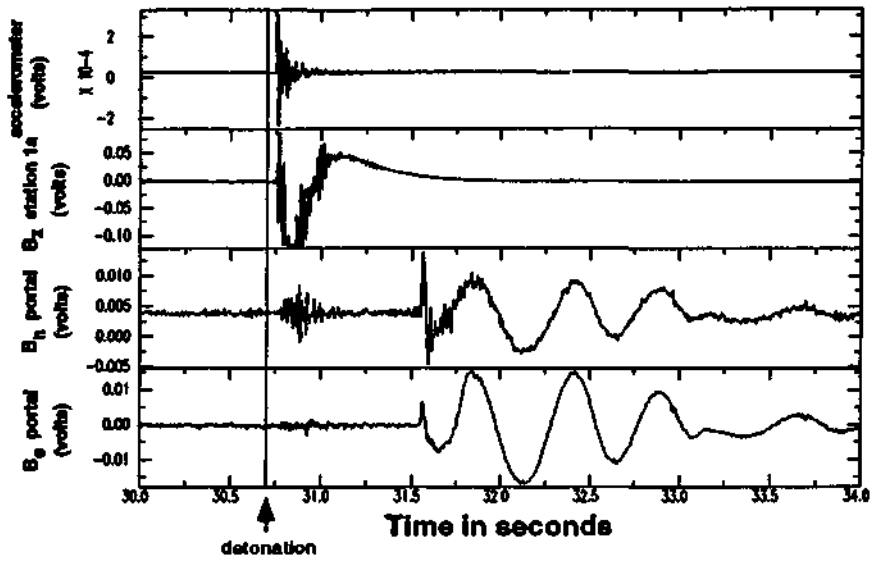

Figure 8. Signals recorded during the first Linchburg mine explosion on March 29, 1996. The detonation time is indicated by the line and arrow at an elapsed time on the record of about 30.7 seconds. Surface ground motion arrived at the 1a site first (top two traces, of the accelerometer and the magnetometer). Ground motion arrived about 0.04 seconds later at the portal, as seen by the more attenuated signals recorded by the two magnetometers in the bottom two traces. The large, low-frequency signal seen starting at about 31.6 *s* elapsed time is from the air wave as it exits the portal.

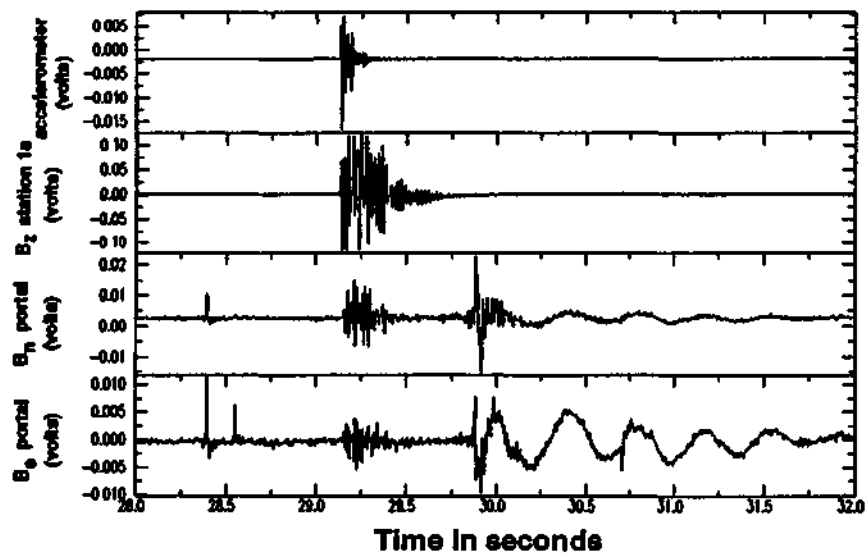

Figure 9. Signals recorded during the third Linchburg mine explosion on April 12, 1996. The detonation time is not shown here, but the surface ground motion arrives at the 1a site first (top two traces, of the accelerometer and the magnetometer). As seen in Fig. 8, ground motion arrives about 0.04 seconds later at the portal. The large, low-frequency signal related to the air pulse arriving at the portal is again seen for this explosion.

The lack of an EMP from the smaller explosions is not surprising, but it is a little surprising that an EMP was not seen for the 2000 kg shot. Lack of a signal certainly indicates that there is not an EMP enhancement when the explosion takes place in a cavity. An additional possibility is that with decreased coupling, there is less fracturing of fresh rock around the explosion. If production of the EMP is related to fracturing of fresh rock, we would expect to see a smaller EMP from a more poorly-coupled explosion. I will examine this question further in the next section.

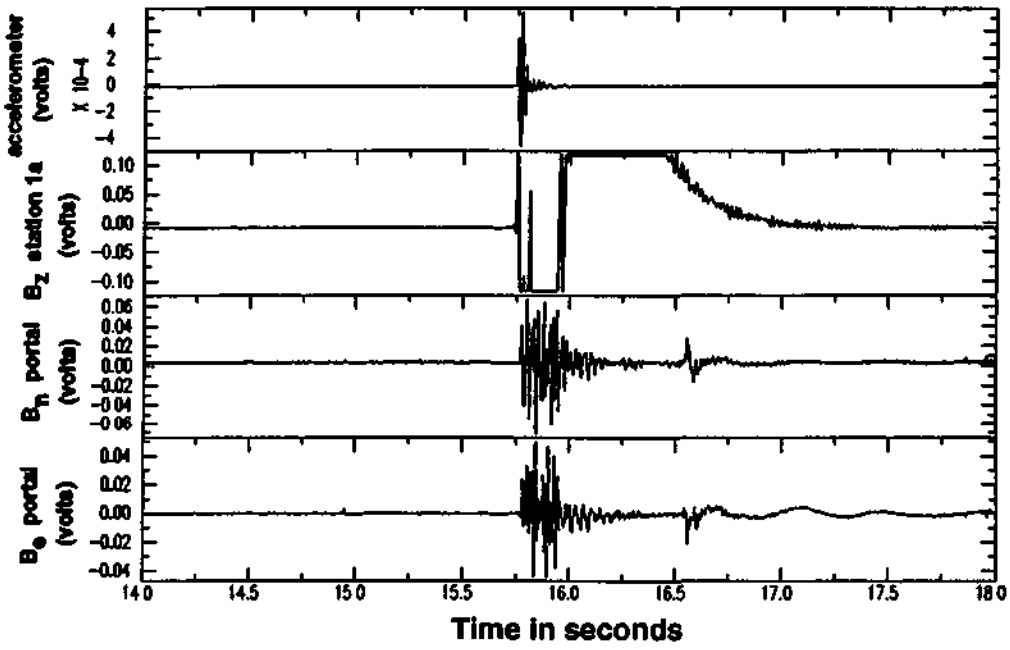

Figure 10. Signals recorded during the second Linchburg mine explosion on April 4, 1996. The detonation time is not shown here, but the surface ground motion arrives at the 1a site first (top two traces, of the accelerometer and the magnetometer). As seen in Figs. 8 and 9, ground motion arrives about 0.04 seconds later at the portal. The smaller amplitude of the later air pulse in this figure is a scaling effect; the ground motion signals are much larger because of size of the detonation.

Rock Fracture as a Source of EMP

Introduction

In a previous review (Sweeney, 1995), I noted that the cause of the EMP could be very different for chemical and nuclear explosions. The character of the EMP also depends on whether the explosion is contained underground or occurs at or above the earth's surface. Certainly, the presence of Compton electrons produced by the gamma radiation of a nuclear explosion (Longmire, 1978; Longmire, 1981; Wouters, 1989) provide one mechanism for EMP not available from a chemical explosion. This is the most probable source of the relatively high-frequency, short-lived pulse that distinguishes the EMP from underground nuclear explosions from the EMP of a concentrated single-shot underground chemical explosion like the NPE (see Sweeney, 1995 and Fig. 11

below). However, this does not rule out the possibility that other sources, common to both nuclear and chemical explosions, may also be present, especially manifest as the lower-frequency, long lived signals seen after the short pulse in nuclear explosions and during the main part of chemical explosions. For example, Wouters (1989) and Malik et al. (1985) suggest that ground motion beyond the region of cavity formation can create a magnetohydrodynamic wave (the seismoelectric effect of Malik and others) that can also be a source of EMP. Adushkin et al. (1995) suggest that an EMP could be caused by rock fracturing. Making a positive identification and characterization of these different sources of EMP from explosions is a very difficult problem that lies beyond the scope of this study, but below I discuss some findings from the literature concerning rock fracturing as a source of EMP and look at the possibility of hydrofracturing as a source of the EMP from the NPE underground chemical explosion.

Over the past 10-20 years there has been continuing interest in electromagnetic radiation associated with fracture of materials in the field of materials science and from the study of "earthquake lights" (light emission at the earth's surface associated with earthquakes). Emission of electrons, positive ions, and photons from rock undergoing fracture have been reported by Brady and Rowell (1986), Cress et al. (1987), Dickinson et al. (1981), Enomoto and Hashimoto (1990), and Khatiashvili and Perel'man (1989) among others. Most of these authors suggest, as Adushkin et al. (1995) do, that as a fracture develops and advances, there is a charge separation on each face of the fracture. It is this charge separation that produces the electric and magnetic fields which may be large enough locally to cause emissions of charged particles and discharges of current. O'Keefe and Thiel (1995) and Adushkin et al. (1995) have advanced models to allow computation of the charge separation effect. Enomoto and Hashimoto (1990) suggest that a massive failure occurring at ground level with a one second duration could produce a total electric charge comparable to that of a bolt of lightning. A laboratory study done on rock samples by Yamada et al. (1989) showed that an EMP was associated with 10-20% of the acoustic emissions occurring during fracturing and that tensile cracks were more efficient than shear cracks at generating EMP. Yamada et al. suggest that production of new cracks may be a necessary condition for EMP. Chen et al. (1990) noted a change in local resistivity near a borehole associated with a hydrofracture experiment. (In a hydrofracture, fluid is forced into a borehole under pressure until the pore pressure is large enough that the rock fails in tension and a fracture parallel to the greatest principal stress direction forms.) The change in resistivity interpreted by Chen et al. (1990) during a hydrofracture was based on an observation of a very low frequency voltage change and could be interpreted as a low frequency EMP.

Fracturing is a well-known and commonly-occurring process in both underground nuclear and chemical explosions (Borg, 1973; Lamb, 1988; Nilson et al., 1991). Borg noted that fracturing around an underground nuclear explosion is anisotropic; fractures extend farther out from the explosion cavity above the working point than below it. Lateral variations in rock properties and the regional stress field would also cause asymmetry in fracture patterns. Nilson et al. point out that there is enough gas pressure in the cavity that "...hydrofractures can break out during the dynamic ground motion and reach significant lengths, even though they are eventually closed by rebound...". Because of the higher potential to produce condensable gases, underground chemical explosions may be even more prone to produce hydrofractures than underground nuclear explosions. Hydrofractures can extend to over 3 times the cavity radius; for a 10 kiloton explosion this could be as much as 90 to 150 m.

Pressure Data from the NPE

One way to assess the potential for hydrofracturing from a chemical explosion, such as the NPE, is to look at cavity pressure data. Cavity pressure was measured by Heinle et al. (1994) during the NPE using steel tubes filled with pressurized water to transmit the pressure signal to a sensor located outside of the explosion cavity. Cavity pressure versus time is compared in Fig. 11 with vertical magnetic EMP signatures seen during the NPE and during Hunter's Trophy, an underground nuclear explosion also detonated on Rainier Mesa at NTS. All three plots use the same time scale, although the EMP data were taken for different events on different dates. As discussed above, the zero-time pulse for the nuclear explosion is of short duration compared to the much broader zero-time pulse (actually slightly delayed) from the chemical (NPE) explosion. The steel tubes used for the cavity pressure measurement were initially pressurized to 10 MPa to prevent them from closing under the high pressure occurring inside the cavity during passage of the hydrodynamic shock wave of the explosion. Because the measurement and recording systems were located about 150 m from the explosion cavity, there was a time delay between the time of the cavity pressurization and when it was recorded. The data in Fig. 11 (bottom set of traces–for each of two sensors) have been corrected for this effect. The dip seen in the pressure data at 0.2 s into the pressure record is a data drop-out and not a real effect. At 0.6 s into the pressure record, falling debris broke the coaxial cable leading to the tunnel portal and the rest of the data were lost. The pressure curves show a rapid increase after detonation and then begin to decline about 0.34 s into the record. Heinle et al. (1994) state that this decline occurs at the time of maximum hydrofracture development, when pressure is relieved due to loss of gas into the fractures. The peak in the pressure curve occurs slightly after the peak in the EMP. The duration of time for which the pressure exceeds 10 MPa probably represents the time for which cavity pressure exceeds hydrostatic, about.25 s. This time roughly matches the duration of the EMP seen during the NPE as shown in the middle plot of Fig. 11. This suggests, but doesn't prove, that the EMP could be related to a period of hydrofracturing.

The uneven shape of the EMP for the NPE in Fig. 11 could be caused by superposition of three or more short pulses which could be caused by discrete hydrofractures. It is interesting to note that the shape of the EMP measured for the NPE is nearly identical at the two different sites where it was measured (see Sweeney, 1994) suggesting a common source function for the EMP. If the EMP is caused by a series of discrete hydrofractures, they would have occurred primarily during the time when cavity pressure was increasing, before the peak pressure, according to Fig. 11.

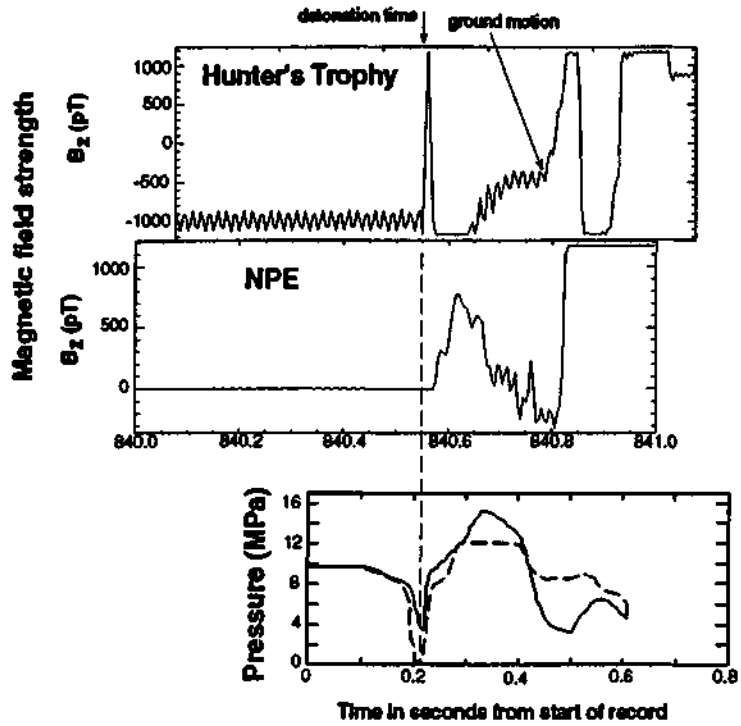

Figure 11. Magnetic pulses recorded at zero-time from a nuclear (top) and chemical (middle) underground explosion and cavity pressure (bottom) measured during the chemical explosion. The two pressure curves (bottom) are from separate sensors, the signal for the dashed curve was saturated during peak pressure. The duration of maximum cavity pressure roughly corresponds to the duration of the magnetic zero-time signal from the chemical explosion (middle trace). The shorter zero-time pulse seen for the nuclear explosion (top trace) is probably related to Compton electrons produced by gamma radiation.

Lost Hills Hydrofrac Experiment

We decided to test the hydrofracture source theory by carrying out low-frequency electromagnetic measurements during a borehole hydrofracture operation. With the cooperation of Pinnacle Technologies, a company that provides fracture monitoring service to the oil industry, we were able to carry out EMP measurements during a commercial hydrofrac operation in an oilfield near Lost Hills, CA. Access to the site and additional free support was provided by Cal Resources, the owner of the well being used, and Haliburton Services, a geophysical service company which provides the monitoring data.

Two sets of horizontal magnetometers were placed on the ground surface at two sites, located about 20 m and 30 m respectively, from the borehole in which the hydrofrac took place. The hydrofacture was to occur at a depth of about 610 m (2000 ft) and the fracture would extend about 100 m above and below the fracture initiation point and about 100 m radially out from the borehole. The closest magnetometer site was located along the azimuth of the expected fracture propagation direction; the other site was located along an azimuth perpendicular to that of the first site. The large number of pipes and other metal structures in the area, local vehicle traffic, and other site limitations prevented us from fielding any telluric lines for this experiment. Data was sampled at 250

samples/s with a Reftek digitizer.

Pressure data from the hydrofracture experiment, provided by Haliburton and Pinnacle Technologies, is shown in Fig. 12. The total period of hydrofracture lasted about 20 minutes—the time of relatively constant peak pressure. The fracture is initiated during the first minute, when pressure rises rapidly. The 20 minute period of relatively constant pressure marks the stage in which the fracture propagates outward, at a speed of a few feet/min. This speed is several orders of magnitude slower than the case for an explosion, when hydrofractures propagate at about half the Rayleigh wave speed of the rock (Nilsen et al., 1991). The pressure at the end of the hydrofrac phase is several hundred psi higher than the initial pressure because of the long time it takes for the pressure to bleed off from the fracture.

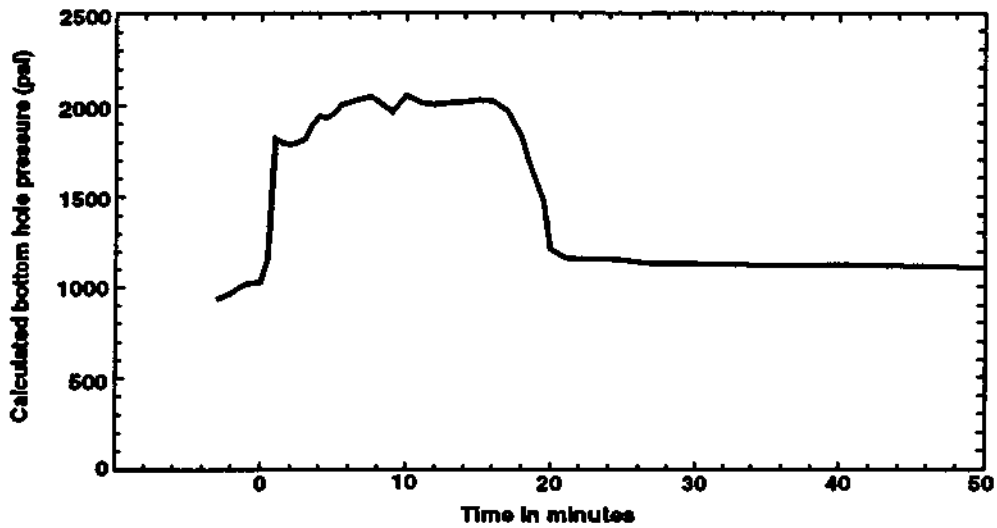

Figure 12. Pressure at the bottom of the borehole (calculation based on measured surface pressure and length of hydrostatic column in the well) during the last phase of the hydrofracture. The fracture is initiated during the initial rapid rise in pressure. Fracture extension occurs during the 20 minutes when the pressure varies between 1800 and 2100 psi.

Figures 13 and 14 show the magnetometer signals recorded during the hydrofrac at sites 1 and 2, respectively. The minute markers at the bottom of each figure show times corresponding to Fig. 12 so that the data can be cross-referenced to the pressure data. At first we thought that the spikes in the data might be related to hydrofracturing, but there is no associated seismic signal, and similar spikes are also seen in data taken several hours before the hydrofrac operation began, as shown in Fig. 15. These spikes are actually changes in the 60 Hz background noise and are probably caused by local power demand fluctuations. In fact, the background noise (not the peak) at this location is about 100 times that of a relatively quiet site. The main source of noise is from local power lines (60 Hz) in spite of the extensive notch filtering we used in the pre-amplifier. Pumps and derricks from nearby producing oil wells and heavy equipment used in the hydrofrac process provide additional sources of EM noise. Obviously, the high level of background noise has masked any signals that may have been produced during underground fracturing; the results of this experiment are inconclusive.

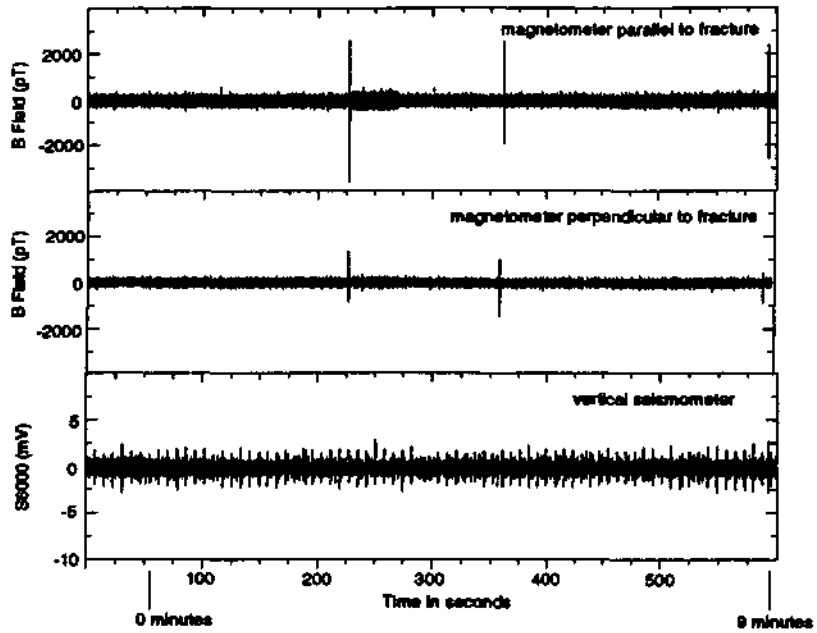

Figure 13. Magnetic (upper two traces) and seismic (bottom trace) signals recorded during the hydrofrac experiment at Lost Hills at site 1. Times in minutes at the bottom of the figure correspond to times shown in Fig. 12.

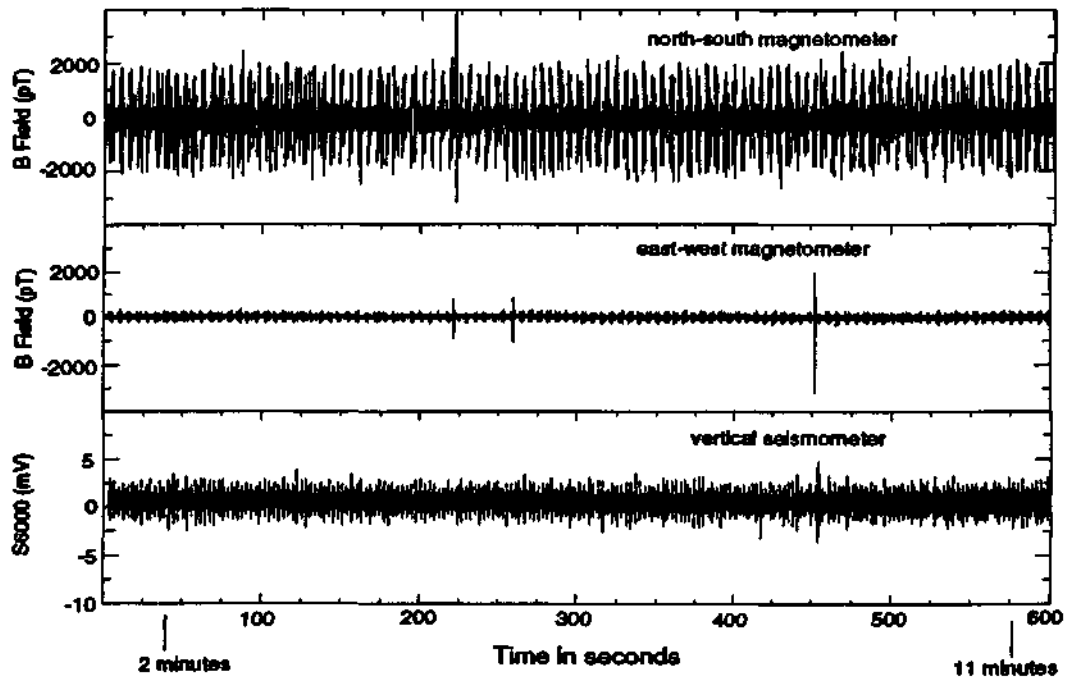

Figure 14. Magnetic (upper two traces) and seismic (bottom trace) signals recorded during the Lost Hills hydrofrac experiment at site 2. Times in minutes at the bottom of the figure correspond to times shown in Fig. 12.

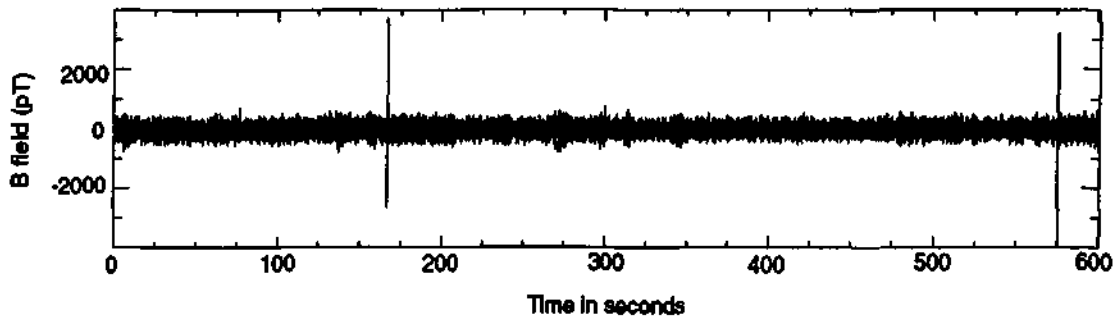

Figure 15. Magnetic field signal recorded at site 2 three hours before the start of the hydrofrac operation. Signal spikes similar to those seen in Fig. 13 and Fig. 14 are also seen here and are probably power system noise.

Efficacy of Low-Frequency EM Measurements for Zero-Time Discrimination of Nuclear and Chemical Explosions

Confidence-building measures are called for in Article IV, Section E, of the Comprehensive Test Ban Treaty with the purpose of "...timely resolution of any compliance concerns arising from possible misinterpretation of verification data relating to chemical explosions...". Low frequency EM measurements taken during the NPE (Sweeney, 1994) suggested that EMP measurements had great potential for use in discrimination. Because the EMP occurs at the time of detonation and must be measured within a few km of ground zero, it cannot be used as part of the remote monitoring system for underground explosions (although it could be used in such a capacity for atmospheric explosions), but it can be considered for use in confidence building. In such use, a country could invite an observation team to carry out low frequency EM measurements during a large, announced underground or surface explosion to help assure the international community that nuclear testing was not taking place directly below the declared explosion.

The purpose of the low frequency EM research program at LLNL has been to learn as much as possible about low frequency EM phenomena associated with underground nuclear and chemical explosions. Our work at LLNL has concentrated on low frequency EMP (< 100 to 200 Hz) because the signals can be detected at greater distances than high frequency EMP; thus they are potentially much less intrusive. In this section I summarize what is known about low frequency EMP from underground nuclear and chemical explosions and above-ground chemical explosions and make assessments about the usefulness and limitations of such measurements for real-time discrimination in the context of the CTBT.

Some of the important features of low frequency EMP from underground nuclear and chemical explosions can be seen in Fig. 16, which was compiled from data acquired by LLNL during the past ten years. Figure 16 shows a series of traces, which are recordings of the vertical magnetic induction field, from six underground nuclear tests (top seven traces) and from one underground chemical explosion (the NPE–bottom two traces). Sampling rates for these waveforms are either 100 Hz or 200 Hz, thus the time resolution is 5-10 ms. The name of each explosion test is listed next to each trace along with the slant range distance of the sensors from the detonation. The total

time span of the traces is 2 s for each trace; thus the arrival of shock wave ground motion (which causes saturation of the digitizer amplifier at the closest sites) is only seen for measurements where the magnetometer was 3.1 km or less from the explosion. Arrival of the ground motion at the sensor 0.3 to 1.2 seconds after the detonation corresponds to a seismic wave speed of about 2500 m/s. Each trace shows a "zero-time" EMP that occurs within a few milliseconds of detonation time (marked by the vertical line "T0" in the figure) for most of the nuclear explosions and with a slight delay (about 10-15 ms) for the chemical explosion. Except for the Hunter's Trophy 1.25 km trace (second from top), which was clipped by a saturated amplifier, all the zero-time pulses for the nuclear tests have a smooth shape. The zero-time pulse for the chemical explosion has a much more irregular character which, as discussed above, may be related to a different source of the EMP. The EMP is relatively short for the closest measurements and becomes broader as distance increases. This is probably due to dispersion; the higher frequency components are more attenuated than lower frequencies as the EMP travels through the earth. The closest stations have a very large amplitude EMP. Signals from Hunter's Trophy at.5 km distance are about 300 times larger than those from Borate at 3.1 km distance. This is roughly consistent with a field strength decrease as the inverse cube of distance. For greater distances, the signal amplitudes are of the same relative magnitude and don't show a strong distance dependence.

To my knowledge, the data from the NPE is the only measurement of a low frequency EMP from a deeply-buried underground chemical explosion. All of our attempts to detect an EMP from smaller underground explosions (Henderson Mine, Carlin Mine, the Kuchen series, and the Linchburg Mine series—see Sweeney, 1995, and this report) have been negative. This suggests that EMP is not as easily developed (nor as strong) in a chemical explosion as it is for a nuclear explosion. Walker (1970) observed a 10 ms electric field (no magnetic field signal was observed) pulse from above-ground chemical explosions and Adushkin and Soloviev (1996) observed electric field signals in the 100 Hz to 1 MHz range from above-ground and shallowly-buried chemical explosions. O'Keefe and Thiel (1991) observed radio emissions in the audio frequency band during quarry blasting and Tomizawa and Yamada (1995) observed EMP in the MHz range during experiments with dynamite detonations in shallow boreholes. These last two studies concluded that the signals observed were caused by fracturing of fresh rock. Clearly, more experience is needed with low frequency EM from large underground chemical explosions, but such experience in controlled situations is difficult to obtain.

The experience with underground nuclear explosions (see Sweeney, 1989, and Fig. 16) is that a strong EMP signal is usually detected, at least for yields in the 10-100 Kt range and at distances less than 10 km. The EMP is a smooth pulse that looks much different from that of chemical explosion in a similar setting (Fig. 16). The signals seen during the Hunter's Trophy test are very strong, about 200 times background when measured at distances up to 1.25 km from the detonation, although the signal strength drops off very rapidly with distance.

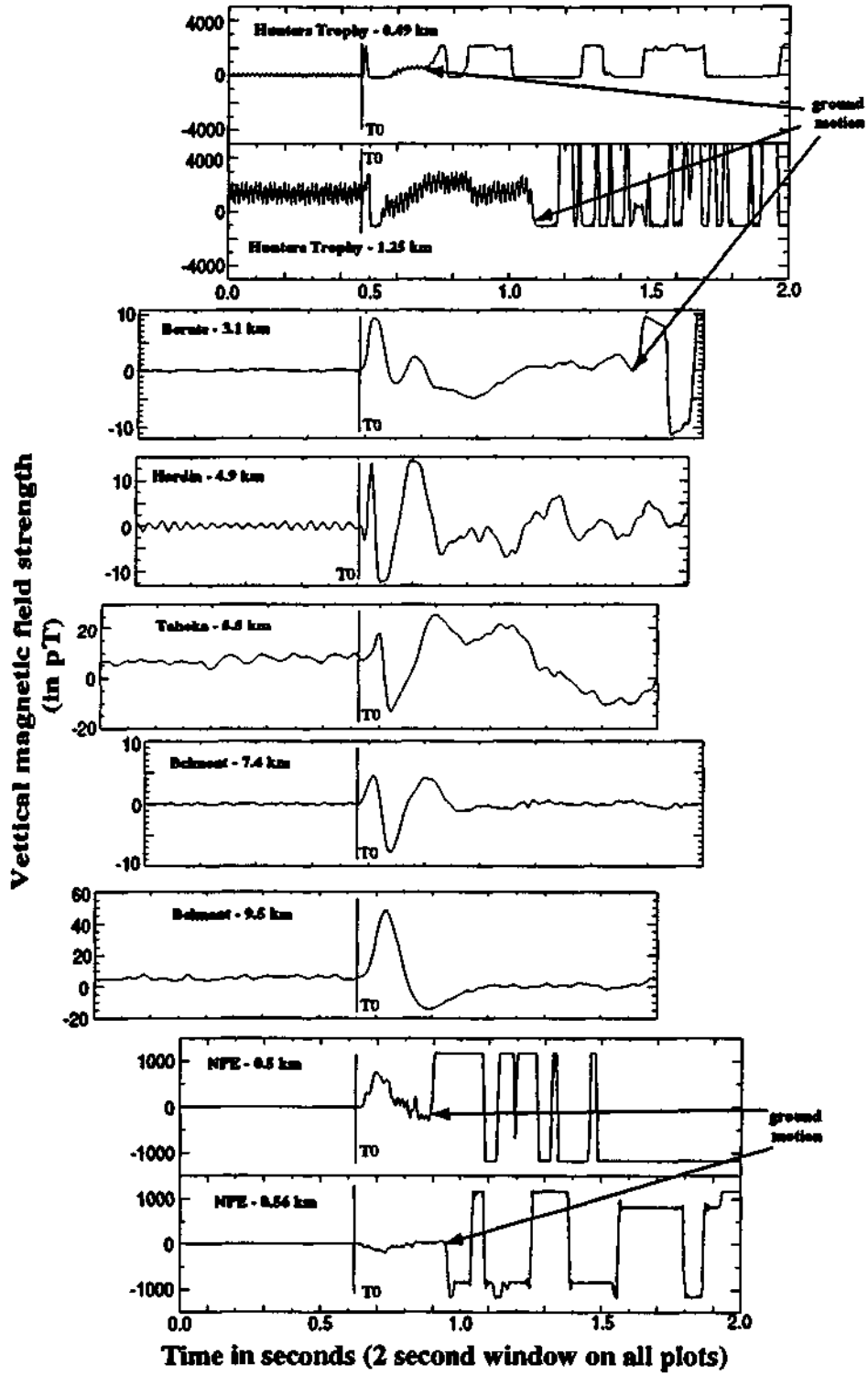

Figure 16. Vertical magnetic field data taken during six underground nuclear explosions (top seven traces) and one underground chemical explosion (bottom two traces). The name of each test and the slant range distance of the magnetometer are indicated. All traces show two seconds of data sampled at 100 to 200 Hz.

Given the above facts, what can we say about the efficacy of low frequency EM measurements for zero-time discrimination? The evidence suggests that a normally-buried underground nuclear explosion of yield 1 Kt or greater will have a high probability of producing a detectable EMP in the 1-30 Hz frequency range. We can not make a similar statement, with similar certainty, for an underground chemical explosion. Our experience suggests that an underground chemical explosion will have a smaller EMP than a similar yield nuclear explosion, if it does happen, and that the pulse shape will be quite different. For similar reasons, masking an underground nuclear explosion with a large surface chemical blast will also be difficult, because the surface blast will probably not create a low frequency magnetic signal and any EMP which develops will probably not be similar to that of an underground nuclear explosion. In conclusion, low frequency EM measurements can be a very powerful tool for zero-time discrimination of yields of 1 Kt or greater, provided that sensors can be placed within 1-2 km of the suspected detonation point in a tamper-proof, low noise environment.

Acknowledgments

This work has benefitted from the long-term (on and off over for nearly ten years) support of the Treaty Verification program at LLNL with funding provided by the DOE Office of Arms Control. Pat Lewis and Don Rock (and, in earlier years, Larry Wethern) have provided invaluable technical support for field data acquisition. The program has also benefitted by having access to seismic data acquisition equipment owned by the Treaty Verification Program and made available for low-frequency EMP research. This work was performed under the auspices of the U.S. Department of Energy by Lawrence Livermore National Laboratory under contract No. W-7405-ENG-48.

References

Adushkin, V. V., V. A. Dubinya, V. A. Karaseva, S. P. Soloviev, and V. V. Surkov, 1995, Generation of low-frequency electric and magnetic fields during large-scale chemical and nuclear explosions: Lawrence Livermore National Laboratory report UCRL-CR-121207, Livermore, CA.

Adushkin, V. V., and S. P. Soloviev, 1996, Generation of low-frequency electric fields by explosion crater formation: Journal of Geophysical Research, v. 101, p. 20,165 - 20,173.

Borg, I. Y., 1973, Extent of pervasive fracturing around underground nuclear explosions: International Journal of Rock Mechanics and Mining Science, v. 10, p. 11-18.

Brady, B. T., and G. A. Rowell, 1986, Laboratory investigations of the electrodynamics of rock fracture: Nature, v. 1321, p. 488-492.

Chen, B.-H., L.-H. Shi, and Y. M. Luo, 1990, A study of the geoelectric effects in the process of hydraulic fracturing experiments: Acta Seismologica Sinica, v. 3, p. 371-382.

Cress, G. O., B. T. Brady, and G. A. Rowell, 1987, Sources of electromagnetic radiation from fracture of rock samples in the laboratory: Geophysical Research Letters, v. 14, p. 331-334.

Dickinson, J. T., E. E. Donaldson, and M. K. Park, 1981, The emission of electrons and positive ions from fracture of materials: Journal of Materials Science, v. 16, p. 2897-2908.

Enomoto, Y., and H. Hashimoto, 1990, Emission of charged particles from indentation fracture of rocks: Nature, v. 346, p. 641-643.

Heinle, R. A., B. C. Hudson, and M. A. Hatch, 1994, Cavity pressure/residual stress measurements from the Non-Proliferation Experiment: in Proceedings of the Symposium on the Non-Proliferation Experiment: M. D. Denney, ed., Department of Energy report CONF-9404100, p. 6.36 - 6.53.

Khatiashvili, N. G., and M. E. Perel'man, 1989, On the mechanism of seismo-electromagnetic phenomena and their possible role in electromagnetic radiation during periods of earthquakes, foreshocks and aftershocks: Physics of the Earth and Planetary Interiors, v. 57, p. 169-177.

Lamb, F. K., 1988, Monitoring yields of underground nuclear tests using hydrodynamic methods: Proceedings of the Conference on Nuclear Arms Technologies in the 1990s, D. Schroeer, and D. Hafemeister, eds., Institute of Physics Conference Proceedings, New York, pp 1-40.

Longmire, C. L., 1978, On the electromagnetic pulse produced by nuclear explosions: IEEE Transactions on Electromagnetic Compatibility, v. EMC-20, p. 3-13.

Longmire, C. L., 1981, EMP from decoupled underground nuclear explosions - final report: Defence Advanced Research Projects Agency report MRC-R-609, Arlington, VA.

Malik, J., R. Fitzhugh, and F. Hormuth, 1985, Electromagnetic Signals from Underground Nuclear Explosions: Los Alamos National Laboratory report LA-10545 MS UC-34, Los Alamos, NM.

Nilson, R., N. Rimer, and E. Halda, 1991, Dynamic modeling of explosively driven hydrofractures: Journal of Geophysical Research, v. 96, p. 18081-18100.

O'Keefe, S. G., and D. V. Thiel, 1991, Electromagnetic emissions during rock blasting: Geophysical Research Letters, v. 18, p. 889-892.

O'Keefe, S. G., and D. V. Thiel, 1995, A mechanism for the production of electromagnetic radiation during fracture of brittle materials: Physics of the Earth and Planetary Interiors, v. 89, p. 127-135.

Sweeney, J. J., 1989, An Investigation of the Usefulness of Extremely Low-Frequency Electromagnetic Measurements for Treaty Verification: Lawrence Livermore National Laboratory report UCRL-53899, Livermore, CA.

Sweeney, J. J., 1995, Low Frequency Electromagnetic Signals from Underground Explosions–On-site Inspection Research Progress Report: Lawrence Livermore National Laboratory, Livermore, CA. report UCRL-ID-122067, July 21, 1995, 22 pp.

Sweeney, J. J., 1994, Low-frequency electromagnetic measurements at the NPE and Hunter's Trophy: a comparison, in Proceedings of the Symposium on the Non-Proliferation Experiment: M. D. Denney, ed., Department of Energy report CONF-9404100, pp. 8.21-8.33.

Tomizawa, I., and I. Yamada, 1995, Generation mechanism of electric impulses observed in explosion seismic experiments: Journal of Geomagnetism and Geoelectricity, v. 47, pp. 313-324.

Walker, C. W., 1970, Observation of the Electromagnetic Signals from a High Explosive Detonation: Lawrence Livermore National Laboratory report UCRL-72150, Livermore, CA.

Wouters, L. F., 1989, The Underground Electromagnetic Pulse: Four Representative Models: Lawrence Livermore National Laboratory report UCID-21720, Livermore, CA, 16 pp.

Yamada, I., K. Masuda, and H. Mizutani, 1989, Electromagnetic and acoustic emission associated with rock failure: Physics of the Earth and Planetary Interiors, v. 57, p. 157-168.

Technical Information Department • Lawrence Livermore National Laboratory
University of California • Livermore, California 94551